



DIE ERDE

Journal of the
Geographical Society
of Berlin

The impact of land use/cover change on extreme temperatures on the Yangtze River Delta, China

Nina Zhu¹, Haiqing Yang^{2,3,*}, Mengyu Zhu⁴, Dahui Li⁵

¹Center for Modern Chinese City Studies & Institute of Urban Development, East China Normal University, Shanghai 200062, China, ninaecnu@126.com

²School of Geographic Sciences, China West Normal University, Nanchong 637009, China

³Sichuan Provincial Engineering Laboratory of Monitoring and Control for Soil Erosion on Dry Valleys, China West Normal University, Nanchong 637009, China, hqyang2021@cwnu.edu.cn

⁴College of Chemical Engineering, Fuzhou University, Fuzhou 350108, China, n190427095@fzu.edu.cn

⁵School of Geospatial Engineering and Science, Sun Yat-Sen University, Zhuhai 519082, China, lidh59@mail2.sysu.edu.cn

*Corresponding author

Manuscript submitted: 7 October 2021 / Accepted for publication: 26 November 2022 / Published online: 23 January 2023

Abstract

The contribution from land use/cover change (LUCC) toward temperature in recent decades is of great concern across the globe. Although there have been many studies, most of them focus on the discussion of average temperature and lack a discussion of extreme temperatures. In this study, we first investigated the spatio-temporal changes in extreme temperatures in the Yangtze River Delta during 1980–2020 using the ensemble empirical mode decomposition (EEMD) method. Then, we explored the impact of LUCC on extreme temperatures using the observation minus reanalysis (OMR) method. Finally, the relationship between the normalized difference vegetation index (NDVI) and extreme temperatures was analyzed using the correlation analysis method. We found that: (1) extreme temperatures have a nonlinear variation characteristics on different time scales. Extremely high temperatures (EHT) clearly exhibited a monthly time scale (quasi-3-month), an interannual time scale (quasi-1-year, quasi-2-year, quasi-3-year and quasi-5-year), and an interdecadal time scale (quasi-10-year and quasi-35-year). Extremely low temperatures (ELT) also clearly exhibited a monthly time scale (quasi-3-month), an interannual scale (quasi-1-year, quasi-2-year, quasi-3-year and quasi-6-year), and an interdecadal scale (quasi-10-year and quasi-20-year). (2) EHT showed an east–middle–west staggered phase and ELT showed a southeast–northwest anti-phase characteristic in spatial distribution. (3) The contribution rates of LUCC on EHT and ELT are 53.6% and 92.4%, respectively, which are higher than for the average temperature (40%). (4) The monthly time scale response of the NDVI to extreme temperatures is more regionally concentrated and significant than that on the interannual time scale in spatial distribution. This paper makes up for the insufficiency of the impact of land use/cover changes on extreme temperature changes at multiple time scales and enriches our understanding of climate change.

Nina Zhu, Haiqing Yang, Mengyu Zhu, Dahui Li 2023: The impact of land use/cover change on extreme temperatures on the Yangtze River Delta, China. – DIE ERDE 153 (4): 219–238



DOI:10.12854/erde-2022-590

Zusammenfassung

Unser Beitrag zu Landnutzungs- und -bedeckungsänderungen (LUCC) zur Temperaturentwicklung in den letzten Jahrzehnten ist weltweit von großer Bedeutung. Obwohl es viele Studien gibt, konzentrieren sich die meisten von ihnen auf die Erörterung der Durchschnittstemperatur und lassen eine Erörterung der Extremtemperaturen vermissen. In dieser Studie untersuchten wir zunächst die räumlich-zeitlichen Veränderungen der Extremtemperaturen im Yangtze-Flussdelta im Zeitraum 1980–2020 mit Hilfe der Methode der Ensemble Empirical Mode Decomposition (EEMD). Dann untersuchten wir den Einfluss von LUCC auf die Extremtemperaturen mit Hilfe der Beobachtung minus Reanalyse (OMR) Methode. Schließlich wurde die Beziehung zwischen dem normalisierten Differenzvegetationsindex (NDVI) und der Extremtemperatur mit Hilfe der Korrelationsanalysemethode analysiert. Wir fanden heraus, dass: (1) Die Extremtemperatur hat nichtlineare Variationsmerkmale auf verschiedenen Zeitskalen. Die extrem hohen Temperaturen (EHT) wiesen eindeutig eine monatliche Zeitskala (quasi drei Monate), eine interannuelle Zeitskala (quasi ein Jahr, quasi zwei Jahre, quasi drei Jahre und quasi fünf Jahre) und eine interdekadische Skala (quasi zehn Jahre und quasi 35 Jahre) auf. Die extrem niedrigen Temperaturen (ELT) wiesen ebenfalls eindeutig eine monatliche Zeitskala (quasi 3 Monate), eine interannuelle Skala (quasi ein Jahr, quasi zwei Jahre, quasi drei Jahre und quasi sechs Jahre) und eine interdekadische Skala (quasi zehn Jahre und quasi 20 Jahre) auf. (2) EHT zeigte eine Ost–Mitte–West gestaffelte Phase und ELT zeigte eine Südost–Nordwest Gegenphasencharakteristik in der räumlichen Verteilung. (3) Der Beitrag von LUCC zu EHT und ELT beträgt 53,6% bzw. 92,4% und ist damit höher als bei der Durchschnittstemperatur (40%). (4) Die Reaktion des NDVI auf Temperaturextreme auf der monatlichen Zeitskala ist regional konzentrierter und signifikanter als die auf der interannualen Zeitskala der räumlichen Verteilung. Diese Arbeit gleicht die unzureichende Untersuchung der Auswirkungen von Änderungen der Landnutzung/Bodenbedeckung auf extreme Temperaturänderungen auf mehreren Zeitskalen aus und bereichert unser Verständnis des Klimawandels.

Keywords Yangtze River Delta, extreme temperature, land use/cover change, contribution rate, ensemble empirical mode decomposition, observation minus reanalysis

1. Introduction

Recent studies have revealed that anthropogenic forcing due to land use/cover change (LUCC) is one of the important factors for the temperature change in recent decades (IPCC 2013; Gogoi et al. 2019). As a purposeful and conscious activity of humankind, LUCC runs through the entire historical process of the continuous development of human society and is an important way for humankind to change the terrestrial ecosystem. LUCC affects not only the exchange of energy, momentum, and matter between the atmosphere and the Earth's surface but also the diversity of terrestrial ecosystems (Turaner et al. 1993). With the intensification of global warming, the frequency of extreme weather and climate events is also rapidly increasing (Luber and McGeehin 2008). In the summer of 2016 alone, many regions of the world experienced the top three extremely high temperature heat waves in history (Nori-Sarma et al. 2019). A large number of studies have confirmed that the human-made effect has been detected in extreme weather events that have occurred (Tebaldi et al. 2006; Orłowsky and

Seneviratne 2012; Sun et al. 2014). For example, Sun et al. (2014) found that the heat-wave that occurred in eastern China in the summer of 2013 was contributed to by human activities, and, if the warming continues to intensify, this kind of heat-wave will occur once a year in the future. As an important external forcing factor of human activities affecting climate, does LUCC have a certain impact on extreme temperatures? What is the magnitude and mechanism of the impact? These questions are worthy of in-depth study and thought. Therefore, exploring the influence of LUCC on extreme temperatures has important scientific significance for an in-depth understanding of the causes of climate change.

In recent years, many scholars have begun to pay attention to the effect of LUCC on extreme temperatures. From the perspective of numerical simulation, Avila et al. (2012) used global models to explore the effect of LUCC on various extreme temperature indices, and they pointed out that on a regional scale, LUCC can be compared with the effect of CO₂. Based on the work of Avila et al. (2012), Pitman et al. (2012) used multiple

models to verify their results, emphasizing the effect of LUCC on extreme temperatures. However, the results of the LUCC extreme climate effects based on the global climate model are very dependent on the model's ability to describe the global and regional climate, and the numerical simulation method requires a large amount of data and is computationally complex, making it difficult to study some data-deficient areas. Other scholars have also confirmed the potential impact of LUCC on extreme temperatures from the perspective of statistical models. For example, *Hu et al.* (2010) used the observation minus reanalysis (OMR) method to separate the signal of LUCC in extreme temperature changes in China, also pointing out that LUCC has a significant impact on extreme temperatures and that about 1/3–1/2 of the nighttime temperature warming trend can be calculated using LUCC. *Teuling et al.* (2010) used satellite data to compare the temperature differences between grasslands and forests during two extreme heatwave events in the summers of 2003 and 2006. They found that the temperature of grassland was 1.7–3.5K higher than that of forest in two cases, which also explained the possible influence of LUCC on extreme temperatures. In addition, some scholars have also conducted related research on how changes in LUCC or LUCC-related parameters lead to extreme temperature changes (*Davin et al.* 2014; *Wilhelm et al.* 2015). Looking at previous studies, there are still insufficient studies on the impact of LUCC on extreme temperatures in China, especially in the Yangtze River Delta region.

The Yangtze River Delta is an area with a high degree of economic development in the eastern coastal area of China. Located in the subtropical monsoon zone, with a wide water area and superior climate and environment, it has always been an ideal place for humans to live. However, as the impact of human activities on the natural environment continues to deepen, especially since the reforms and opening up, it had only taken the region about 30 years to complete the urban development and construction that Western countries had completed over hundreds of years (*Tang et al.* 2021). With the rapid development of the urban area, the land use/cover in this region has undergone tremendous changes, which has an important influence on the regional microclimate, leading to frequent extreme climate events. Relevant studies point out that the highest extreme temperatures in the Yangtze River Delta has been 39.24°C (2013), the lowest has been 34.25°C (1982), the maximum number of high temperature days is 34.6 days (2013), and the minimum has

been 2.91 days (1982) (*Sang* 2012). The extremely high temperature index was in a downward trend before the 1980s and began to rise after the 1990s, entering a period of frequent high temperatures (*Sang* 2012). The frequent occurrence of extreme climate events has brought huge economic losses to the region. In addition, previous studies have highlighted the impact of LUCC on temperature. However, most of them focus on the effect of LUCC on average temperature, and the effect of LUCC on extreme temperatures is not well explored. Therefore, studying the changing laws of extreme climate events in the region and clarifying the contribution rate of LUCC to extreme temperatures is of great significance for dealing with extreme climate events and rationally planning land use.

For the above reasons, we attempted to explore the spatio-temporal dynamics of extreme temperatures in the Yangtze River Delta and assessed the spatial heterogeneity of the influences of LUCC on temperature. Based on observed temperature data at 68 meteorological stations during the period of 1980–2020, we first investigated the spatio-temporal changes and periodic of extreme temperatures by using the ensemble empirical mode decomposition (EEMD; see Section 2.2.3) and empirical orthogonal function (EOF) methods; then we analyzed the spatio-temporal changes of LUCC by using land use transfer matrix method; finally, we investigated the contribution rates of LUCC toward extreme temperatures and the correlation between the normalized difference vegetation index (NDVI) and extreme temperatures on different time scales by using the observation minus reanalysis (OMR) method and correlation analysis method. The results have certain reference significance for the relevant departments to formulate policies on urban development, natural disaster prevention and environmental protection in the region.

2. Materials and methods

2.1 Study area and data resources

The Yangtze River Delta in this study includes four provinces: Jiangsu Province, Anhui Province, Zhejiang Province, and Shanghai (*Fig. 1*). It is located in eastern China and lies between 114°54' and 122°42' E and 27°12'–35°20' N. The region is under a monsoon climate regime with four distinct seasons. The annual precipitation is about 1000 mm, of which the precipitation in summer accounts for two-thirds of

The impact of land use/cover change on extreme temperatures on the Yangtze River Delta, China

the total precipitation (Gu et al. 2011). The average temperature is close to 30°C in July and August, and the maximum temperature recently exceeded 40°C in Shanghai (Gu et al. 2011). The high terrain is in the north and south and the low terrain is in the middle, which is dominated by plains and hills. The superior geographical location and suitable climatic conditions have made the region's economic development level and human activity intensity relatively high, leading to huge changes in land use patterns, which has an important impact on the regional climate, especially the temperature (Yang et al. 2021). On a global scale, the temperature is mainly affected by factors such as atmospheric circulation, volcanic eruptions, and sunspots. However, on the regional scale, the temperature is mainly affected by surface properties and human activities.

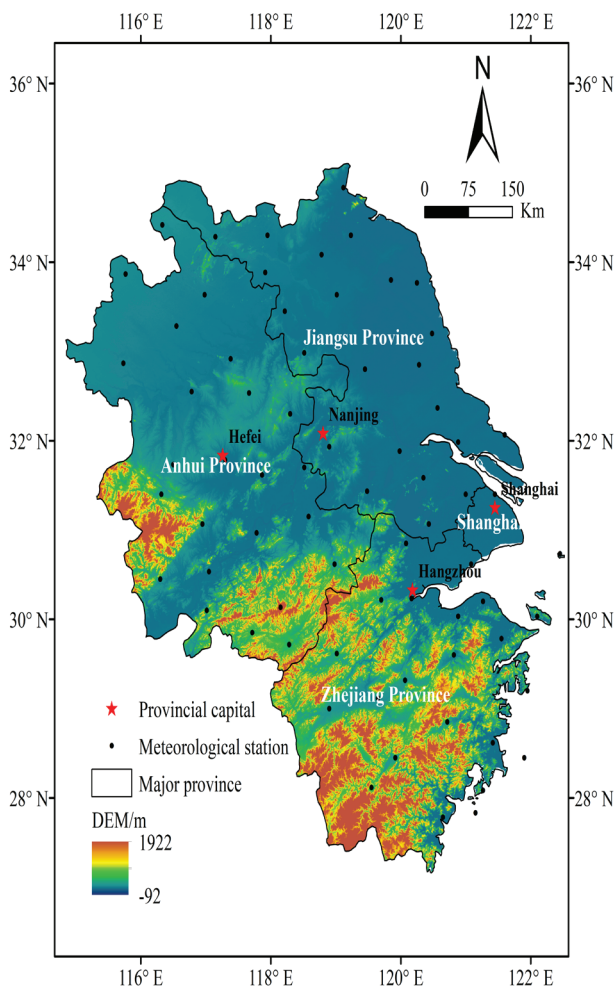


Fig. 1 Study area and spatial distribution of 68 meteorological stations. Source: own elaboration

The time span of this study was 1980–2020. The observed daily temperature (including daily maximum temperature and daily minimum temperature) of 71 meteorological stations was obtained from the *China Meteorological Data Service Center (China Meteorological Administration 2011)*. As the data of three meteorological stations have only been recorded since 2010, discounted them for this study. Finally, the data of the remaining 68 meteorological stations were obtained, and the geographical locations of each station are shown in *Figure 1*. The reanalysis monthly temperature datasets were obtained from the National Center for Environmental Prediction/National Center for Atmospheric Research (NCEP/NCAR) (Kistler et al. 2001), with a spatial resolution of $2.5^{\circ} \times 2.5^{\circ}$. The reasons for choosing NCEP/NCAR Reanalysis data are as follows: there are four types of reanalysis dataset commonly used in climate research, namely, NCEP/NCAR R1, the National Center for Environmental Prediction/Department of Energy (NCEP/DOE) R1, the European Center for Medium-Range Weather Forecast (ECMWF) reanalysis data (ERA), and the Japan Meteorological Agency (JMA) reanalysis data (JRA). In this four kind of reanalysis data, NCEP/NCAR R1 contains the least surface observation data in the assimilation process; the NCEP/DOE R2 corrected some errors in the NCEP/NCAR R1, but it also contains more surface observation data; ERA-40 and JRA-25 use more surface observation data than the NCEP, and their quality and reliability are relatively high, but the signal strength is weaker than for the NCEP. Therefore, NCEP/NCAR R1 is the most widely used. The NDVI is from the National Science and Technology Information (*The National Center for Atmospheric Research 2018*), with the temporal resolution by month and the spatial resolution of $8 \times 8 \text{ km}^2$. The LUCC dataset during the period of 1980–2015 of the Yangtze River Delta was derived from the Resource and Environmental Science Data Center (RESDC) (Xu 2018), with a spatial resolution of $1 \times 1 \text{ km}$. The LUCC dataset during the period of 2016–2020 of the Yangtze River Delta was derived from the National Aeronautics and Space Administration (Friedl and Sulla-Menashe 2015), with a spatial resolution of $0.05^{\circ} \times 0.05^{\circ}$.

Before quantitative analysis, we performed the following processing for the dataset. First, as the spatial resolutions of LUCC in 1980–2015 and 2016–2020 were inconsistent, we adopted the resampling method in the ArcGIS 10.5 software to reduce the spatial resolution of 2016–2020 to $8 \times 8 \text{ km}^2$, making it consistent with the spatial resolution for the period of 1980–

2015. The monthly NDVI spatial distribution dataset is based on a continuous time series of the moderate resolution imaging spectroradiometer (MODIS) NDVI satellite remote sensing data. Using the maximum value composite (MVC) method, we generated the monthly and annual NDVI dataset from 1980 to 2020 with a spatial resolution of $8 \times 8 \text{ km}^2$. Finally, to analyze the impact of LUCC on extreme temperatures, we used ArcGIS 10.5 software to extract the values of the NCEP/NCAR reanalysis dataset and the monthly and annual NDVI values corresponding to each station, based on 68 meteorological stations.

2.2 Methodology

The framework of this study is shown in *Figure 2*, and it shows the relationship between the various methods and their effects.

2.2.1 Extreme temperature index

There are different extreme temperature indices established in the field of meteorology. In order to accurately describe the changes in extreme temperatures, we selected two of the 27 extreme temperature indices recommended by the Expert Group on Climate Change Detection, Monitoring and Index jointly initiated by the Climate Commission of The World Meteorological Organization and the Climate Variability Prediction Program to represent the change in extreme temperatures. This series of indices can reasonably and effectively characterize extreme climate changes in both observation and simulation studies (*Zhang et al. 2011*). The two extreme temperature indices, belonging to the absolute extreme temperature index, are the monthly maximum value of daily maximum temperature (TXx) and the monthly minimum value of daily minimum temperature (TNn) (*Karl et al. 1999*), and their definitions are as follows:

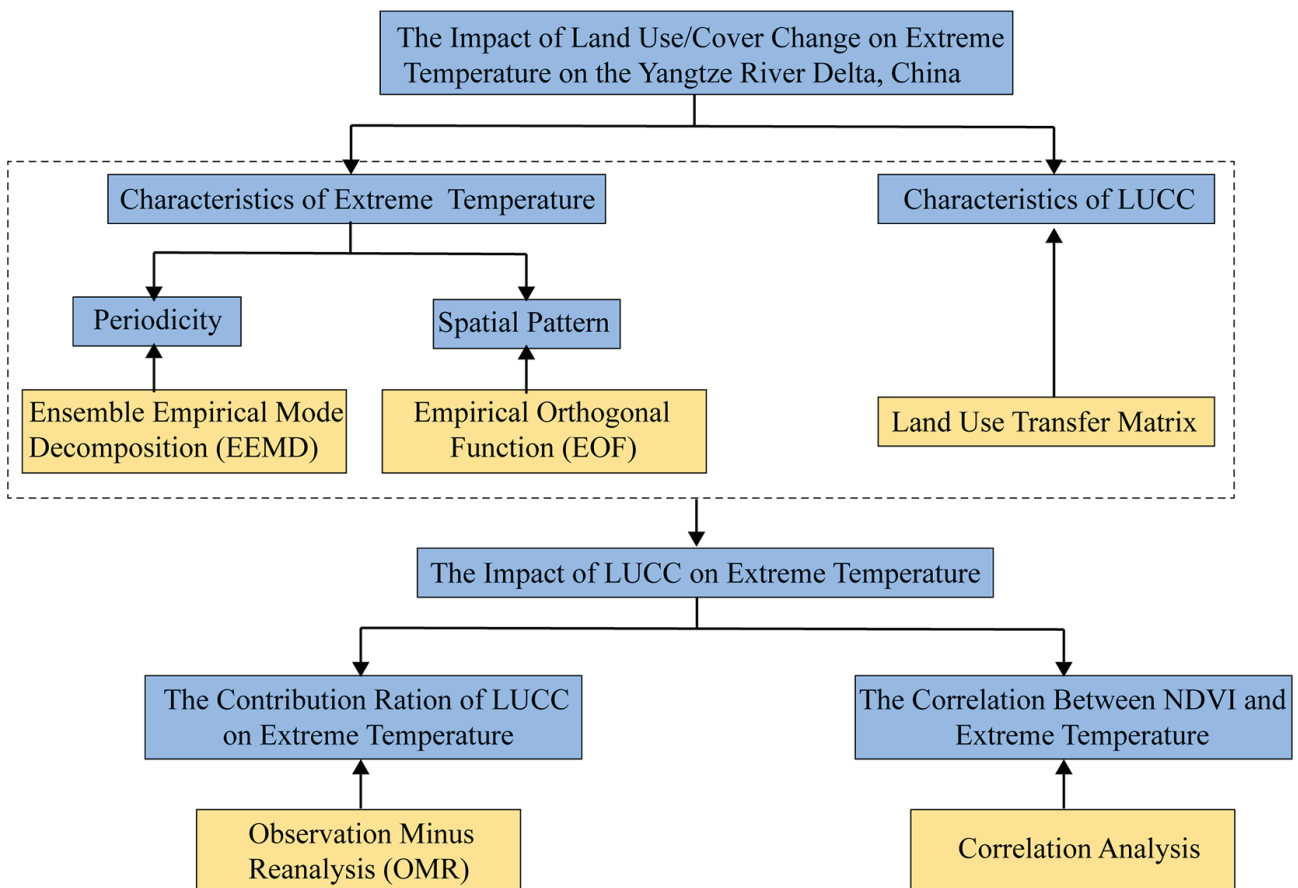


Fig. 2 Framework of the study. Source: own elaboration

Let TX_x be the daily maximum temperatures in month k , period j . The maximum daily maximum temperature each month is then:

$$TX_{x_{kj}} = \max(TX_{x_{kj}}). \quad (1)$$

Let TN_x be the daily minimum temperatures in month k , period j . The minimum daily minimum temperature each month is then:

$$TN_{n_{kj}} = \min(TN_{n_{kj}}). \quad (2)$$

2.2.2 Ensemble Empirical Mode Decomposition

Ensemble empirical mode decomposition (EEMD) is utilized to analyze the nonlinear and periodic characteristics of extremely high/low temperatures. The climate-hydrological system is a complex nonlinear system, which is the result of the interaction of various climate and hydrological elements, and is accompanied by the influence of human activities. This complexity cannot be described by a simple linear relationship. We need to understand the climate-hydrological process from a multi-scale and multi-level perspective. EEMD is a method that can effectively deal with nonlinear and non-stationary problems and can analyze the internal mechanism of elements from multiple time scales. It has been widely used in meteorology.

EEMD is proposed by *Wu and Huang (2011)*, and it is based on empirical mode decomposition (EMD) and improvement of the EMD (*Wu and Huang 2011*). EEMD can adaptively decompose the time-frequency domain, according to the local time variation features, and is completely free from the constraints of the Fourier transform so that it can obtain a high time-frequency resolution (*Wu and Huang 2011*). Therefore, we used the EEMD, which is the best decomposition method to extract the changes of various scales in the temperature signal from the temperature time series. The steps of the EEMD are as follows:

1. White noise with specified amplitude is added to the sequence of the original signal:

$$x_i(t) = x(t) + n_i(t), \quad (3)$$

where $x_i(t)$ is the new signal after adding the white noise, $x(t)$ is the original signal, and $n_i(t)$ is white noise.

2. According to the principle of EMD decomposition, the signal after adding white noise is decomposed to obtain the component IMF1 (the first Intrinsic Mode Function).
3. Adding the same white noise in the sequence that has separated out the IMF1 and repeating the above step can obtain the component IMF2 (the Second Intrinsic Mode Function).
4. Repeating the above steps can result in different IMFs (the Intrinsic Mode Functions) and then using the average of these components as the final result, so that white noise can be eliminated, as shown in the following formula:

$$C_j(t) = \frac{1}{N} \sum_{i=1}^N C_{ij}(t). \quad (4)$$

Where $c_j(t)$ represents $c_{ij}(t)$ the j^{th} component IMF, where N represents the numbers of adding white noise, and represents the j^{th} component IMF after adding the i^{th} white noise.

5. After the above decomposition, different component IMFs and trend items can be obtained, and then the signal can be reconstructed, as shown below:

$$x(t) = \sum_{j=1}^n C_j(t) + r_n(t), \quad (5)$$

where $x(t)$ represents the reconstructed signals, $c_j(t)$ represents the different IMFs, and $r_n(t)$ represents the trend term.

2.2.3 Empirical orthogonal function

The empirical orthogonal function (EOF) method has been used to analyze the main spatial pattern of extremely high/low temperatures in the past 40 years. The characteristics of spatial change are the most basic characteristics of geographic elements or geographic phenomena and are of great significance for understanding the development law and direction of phenomena. EOF is mainly used to extract the characteristics of the main data. It can describe the original variable field with a small number of spatial distribution modes and can cover a large amount of information about the original variable field (*Zhu et al. 2019a*). The method has been widely used in the field of meteorology. Its analysis principle is described below.

Supposing there are spatio-temporal matrix data with a spatial dimension of m and a time dimension of n , then the matrix can be expressed as follows:

$$X_{ij} = \begin{bmatrix} x_{11} & x_{12} & \dots & x_{1n} \\ \vdots & \vdots & \ddots & \vdots \\ x_{m1} & x_{m2} & \dots & x_{mn} \end{bmatrix}$$

$$(i = 1, 2, \dots, m; j = 1, 2, \dots, n). \tag{6}$$

Then, EOF decomposition is to decompose the above matrix into the form of the multiplication of space function and time function, as shown in the following equation:

$$X = VT = \sum_{k=1}^p v_{ik} t_{kj}, l = 1, 2, \dots, m; j = 1, 2, \dots, n, \tag{7}$$

where V represents the eigenvector matrix, and T represents the time vector matrix. According to orthogonality, the above equation must satisfy the following conditions:

$$\begin{cases} \sum_{i=1}^m v_{ik} v_{il} = 1, k = l \\ \sum_{i=1}^m v_{ik} v_{il} = 0, k \neq l \end{cases} \tag{8}$$

Next, we can obtain the eigenvectors, eigenvalues ($\lambda_1, \lambda_2, \dots, \lambda_m$), and time coefficients. By arranging the eigenvalues in descending order ($\lambda_1 \geq \lambda_2 \geq \dots \geq \lambda_m \geq 0$), the variance contribution rate, R_k , of each eigenvector can be obtained:

$$R_k = \frac{\lambda_k}{\sum_{i=1}^m \lambda_i}, k = 1, 2, \dots, p (p < m) \tag{9}$$

2.2.4 Observation minus reanalysis

Observation minus reanalysis (OMR) method is used to explore the contribution rate of LUCC to extremely high/low temperatures. This method is known in estimating the impact of LUCC on the temperature. OMR-based studies have been conducted over various regions across the globe and appear to be successful in capturing the LUCC impact on temperature trends (Wang et al. 2013).

The theoretical basis of the OMR method is that due to the surface temperature in the reanalysis data being different from the observation data, it is only determined by the atmospheric environment, and it is considered to be insensitive to urbanization and underlying surface conditions (Wang et al. 2013). Therefore, the temperature difference between observation data and reanalysis data can reveal the impact of land use/cover change or urbanization on climate change. The contribution rate of OMR is defined as follows:

$$R_{OMR} = \frac{|T_{Reanalysis\ data}|}{T_{Observation\ data} \times 100\%} \tag{10}$$

where R_{OMR} represents the contribution rate of LUCC on temperature, $T_{(Reanalysis\ data)}$ represents the trend of reanalysis data of temperature, and $T_{(Observation\ data)}$ represents the trend of observation data of temperature.

2.2.5 Correlation analysis

Correlation analysis is used to analyze the relationship between extremely high/low temperatures and NDVI on the Yangtze River Delta. This method mainly describes the closeness of the relationship between objective phenomena and expresses it with appropriate statistical indicators that are easy to understand, and it has been widely used in various fields (Zhang and Zhou 2021). The calculation formula is as follows:

$$r = \frac{\sum_{i=1}^n (x_i - \bar{x})(y_i - \bar{y})}{\sqrt{\sum_{i=1}^n (x_i - \bar{x})^2 \sum_{i=1}^n (y_i - \bar{y})^2}} \tag{11}$$

In Equation (11), x_i and y_i represent the values of two variables; \bar{x} and \bar{y} are the average values of the two variables; r is the correlation coefficient, and when $r > 0$, the two variables are positively correlated, whereas, when $r < 0$, the two variables are negatively correlated. A larger $|r|$ indicates a stronger correlation.

3. Results

3.1 Characteristics of extreme temperatures

3.1.1 Periodicity

According to previous studies (Qin et al. 2012; Liu et al. 2019; Zhu et al. 2019b), we know that the average temperature time series has been nonlinear and nonstationary. Therefore, similar with the average temperature, the extremely high temperatures (EHT) and extremely low temperatures (ELT) were decomposed into different time scales by the EEMD method to discover the intrinsic modes in their signal. Matlab 2018a software was used for implementing the EEMD method. The EEMD results of the EHT and ELT time series in the Yangtze River Delta during 1980–2020 are shown in Figure 3. There are four intrinsic mode functions (i.e., IMF1, IMF2, IMF3, and IMF4) and a trend (RES) for the EHT and ELT time series and all

IMFs passed the 95% significance test, which means that each component is the result of a signal with an actual physical meaning. The IMFs represent the oscillation characteristics from high to low frequencies of the original sequence at different scales (the highest frequency is IMF1, followed by IMF2, IMF3, and IMF4) and all have specific physical meanings, while the RES is a monotonic function that presents the overall trend of the temperature time series (Zhu et al. 2019b). Moreover, the oscillation frequency of the EHT and ELT time series is relatively fast on the short change cycle, but the oscillation frequency is relatively stable on the long change cycle.

As shown in Figure 3a and Table 1, EHT has a quasi-3-month (IMF1) cycle on the monthly time scale; quasi-1-year (IMF2), quasi-2-year (IMF3), quasi-3-year (IMF4) and quasi-5-year (IMF5) cycles on the interannual time scale; and quasi-10-year (IMF6) and quasi-35-year (IMF7) cycles on the interdecadal time scale. The trend term (RES) reflects the changes in EHT during 1980–2020 and it increased first during 1980–2008 and then decreased during 2009–2020. According to calculations, EHT increased by 0.56°C per decade during 1980–2008 and decreased by 0.55°C per decade during 2009–2020 (Fig. 3a). Compared with the EHT time series, there are different change characteristics in the ELT time series (Fig. 3b). The ELT time series has a quasi-3-month cycle on the monthly

time scale; quasi-1-year, quasi-2-year, quasi-3-year and quasi-6-year cycles on the interannual time scale; and quasi-10-year and quasi-20-year cycles on the interdecadal time scale. The trend term indicates that ELT has been showing an increasing trend during 1980–2020, and it increased 0.53°C per decade. From the variance contribution rate of the EHT and ELT time series in different components, we can see that the variance contribution rate on the short change cycle is greater than the variance contribution rate on the long change cycle, indicating that the oscillation characteristics on the interannual time scale are the main oscillation characteristics of the EHT and ELT time series. The oscillation periods of EHT and ELT on different time scales are similar, which may be the result of the forcing outside the natural boundary and the internal change of the climate system (Bai et al. 2017). Among them, both EHT and ELT have quasi-2-year and quasi-3-year cycle on the interannual time scale, which is similar to the quasi-2 and 4-year cycle of the atmospheric circulation troposphere (Yao et al. 2014). The quasi-5-year cycle of EHT and the quasi-6-year cycle of ELT are the same as the change periods of ENSO and North Atlantic oscillation. The quasi-10-year cycle and quasi-34-year cycle of EHT and the quasi-10-year cycle and quasi-20-year cycle of ELT correspond to quasi cycle of solar activity with cold and warm phases alternating of the Pacific Ocean (Qian and Lu 2010; Chen et al. 2017).

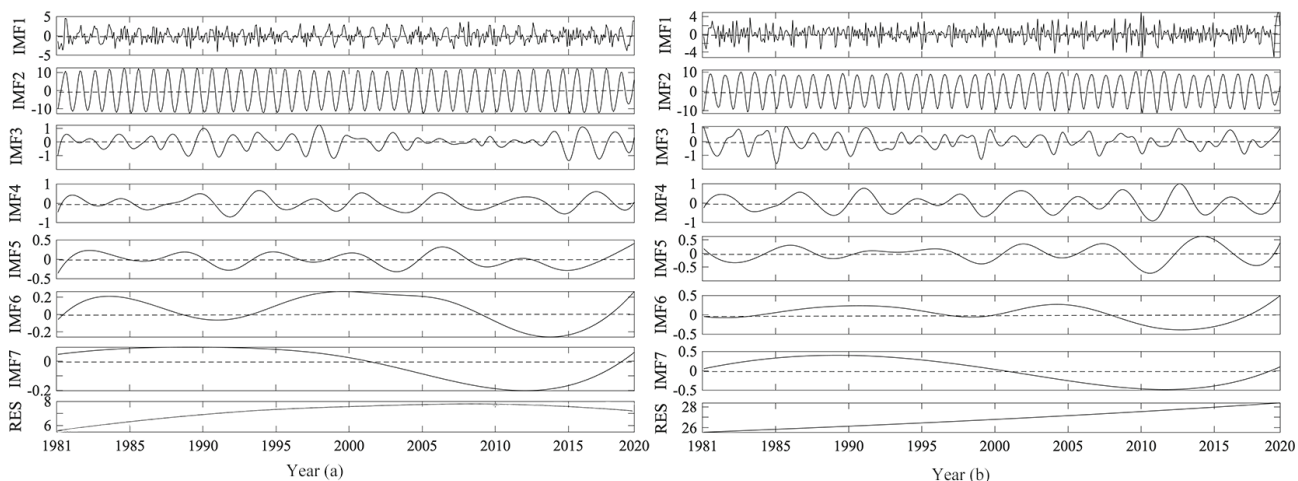


Fig. 3 EEMD result of extremely high temperatures (a) and extremely low temperatures (b) on the Yangtze River Delta during 1980–2020. Source: own drawing based on the research results

Table 1 Cycles of extremely high/low temperatures

Extremely high temperatures (EHT)			Extremely low temperatures (ELT)	
	Cycles	Variance contribution rate (%)	Cycles	Variance contribution rate (%)
IMF1	3	5.37	3	3.48
IMF2	1	91.75	1	95.27
IMF3	2	0.60	2	0.35
IMF4	3	0.39	3	0.14
IMF5	5	0.17	6	0.04
IMF6	10	0.08	10	0.03
IMF7	34	0.21	20	0.02
RES		1.42		0.66

Note: The resolution of IMF1 is monthly, whereas the resolution of IMF2, IMF3, IMF4, IMF5, IMF6, and IMF7 is in years for cycles

3.1.2 Spatial pattern

In order to explore the main spatial pattern of EHT and ELT in the past 40 years, the EOF method was used. The EOF analysis method can decompose the variable field that changes with time into (1) the space function part that does not change with time and (2) the time function part that only depends on a time change and can extract the feature quantity of the main data. Table 2 shows the first seven principal components of EHT and ELT after EOF decomposition and each principal component passed the North significance test (North et al. 1982). When selecting the number of main principal components, we used the 80% standard, i.e., when the cumulative variance contribution rate of the current principal components reaches 80%, it is considered that these principal components are sufficient to represent most of the information of EHT or ELT. It can be seen that the variance contribution rate of the first principal component of EHT was 83.8%, and the principal

component variance contribution rate dropped rapidly from the second component. Therefore, only the spatial eigenvector field corresponding to the first principal component was selected for analysis, and the spatial eigenvector field corresponding to the first principal component is called the first mode (EOF1) and it represents the main spatial pattern of EHT. For ELT, the cumulative variance contribution rate of the first principal component was over 80%, so the first spatial eigenvector field corresponding to the first principal component represents the main information of ELT. The variance contribution rate of the first principal component was 87.2% and greater than the others, so the spatial eigenvector field corresponding to the first principal component is also the main spatial pattern of ELT.

The EOF1 of EHT (Fig. 4a) represents the main spatial pattern and the magnitude of the value reflects the magnitude of the change in EHT. Figure 4a shows that there are both positive and negative values, and the

Table 2 Variance contribution rate and cumulative variance contribution rate of the first seven principal components of EHT and ELT

Extremely high temperatures (EHT)			Extremely low temperatures (ELT)		
Principal component	Variance contribution rate (%)	Cumulative variance contribution rate (%)	Principal component	Variance contribution rate (%)	Cumulative variance contribution rate (%)
1	83.830	83.830		87.169	87.169
2	5.264	89.094		2.185	89.354
3	1.996	91.090		1.718	91.072
4	1.359	92.449		1.696	92.768
5	1.019	93.468		0.952	93.720
6	0.714	94.182		0.771	94.491
7	0.695	94.877		0.690	95.181

The impact of land use/cover change on extreme temperatures on the Yangtze River Delta, China

positive values are mainly distributed in the east and west of the Yangtze River Delta and the negative values are mainly distributed in the middle of the Yangtze River Delta, indicating that the changes in EHT presents an east-middle-west staggered phase spatial pattern. It means that either EHT in the east and west of the Yangtze River Delta has increased while EHT in the middle of the Yangtze River Delta has decreased or EHT in the east and west of the Yangtze River Delta has decreased while EHT in the middle of the Yangtze River Delta has increased in the past 40 years. The high-value center of the positive phase is mainly located in the northeast, southeast, and west of the Yangtze River Delta, indicating that EHT changes in these areas are relatively large. The low-value center of the negative phase is mainly located in Jinhua City.

The EOF1 of ELT (Fig. 4b) represent the main spatial pattern, and the magnitude of the value reflects the magnitude of the change in ELT. Figure 4b has a different spatial pattern to Figure 2a, but there are also

positive and negative values, and the positive values are mainly distributed in the southeast of the Yangtze River Delta and the negative values are mainly distributed in the northwest of the Yangtze River Delta, indicating that the changes in ELT present a southeast-northwest anti-phase characteristic. It means that overall either ELT in the southeast of the Yangtze River Delta has decreased while in the northwest of the Yangtze River Delta it has increased or ELT in the southeast of the Yangtze River Delta has increased while in the northwest of the Yangtze River Delta it has decreased in the past 40 years. The high-value center of the positive phase is mainly located in the southeast corner, indicating that ELT changes in this area are relatively large; the low-value center of the negative phase is located in the northeast corner and Huangshan City. In addition, the numerical range (0.683) of ELT is larger than that of EHT (0.155), which means that the change magnitude of ELT is higher than the change range of EHT, and the change in ELT is more sensitive.

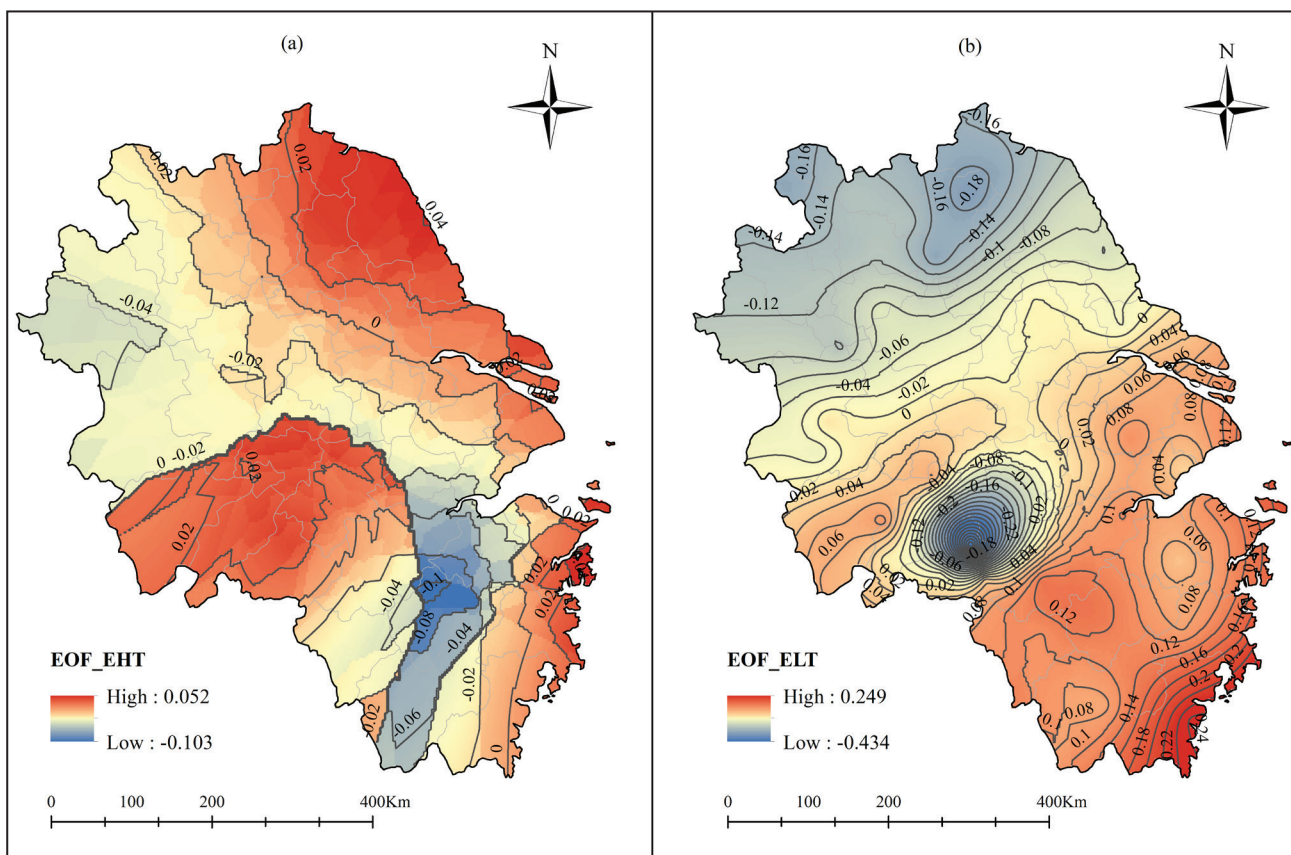


Fig. 4 EOF of EHT and ELT on the Yangtze River Delta during 1980–2020. Source: own drawing based on the research results

3.2 Characteristics of LUCC

With rapid economic development, LUCC has undergone tremendous changes on the Yangtze River Delta. *Table 3* gives the land use changes on the Yangtze River Delta from 1980 to 2020. First, cultivated land has always been the largest proportion of land use in the Yangtze River Delta, followed by woodland, and the unused land is the smallest proportion of land use. Second, the area of cultivated land and grassland decreased by 6.6% and 0.7%, respectively, while the area of woodland, water, construction, and unused land increased by 0.7%, 0.3%, 6.21%, and 0.08%, respectively, from 1980 to 2020. It can be seen that the changes in cultivated land and construction land are the largest, and the decrease in cultivated land is equivalent to the increase in construction land, which means that cultivated land has been mainly converted into construction land on the Yangtze River Delta during the period of 1980 to 2020. In addition, the area ratio of construction land in 2020 was more than twice that of 1980, and the increase in construction land represents the increase in people and the expansion of cities, which means that people have played an important role in land use changes in the last 40 years. The reduction in the total amount of cultivated land has led to a gradual decrease in the per capita cultivated land area. According to calculations, in 2020, the per capita cultivated land area in the Yangtze River Delta was about 0.073 hectares per person, which was lower than the national per capita cultivated land area, indicating that the cultivated land supply and demand contradiction in the Yangtze River Delta is serious.

In addition, from the proportion of land-use type spatial transfer area on the Yangtze River Delta from 1980 to 2020, it can also be seen that the proportion of the cultivated land transferred to construction land is the largest, followed by the proportion of cultivated land transferred to woodland, the proportion of

construction land transferred to cultivated land, and the proportion of woodland transferred to cultivated land. In recent years, China has implemented a policy of returning cultivated land to woodland to improve the ecological environment. The results in *Figure 4* show that this policy has been responded to; however, the proportion of cultivated land transferred to woodland is 3.6%, but 3.0% of woodland has been transferred to cultivated land (*Fig. 5*), meaning that the response to this policy is not obvious.

From the spatial patterns of LUCC in 1980 and 2020 (*Fig. 6*), we can see that the cultivated land is mainly distributed in the north and the woodland and grassland is mainly distributed in the south, with Shanghai and Lu'an as the boundary. This is mainly due to the fact that the northern part of the Yangtze River Delta is mostly hilly and plain and so it is convenient for land development and utilization, while the southwestern part of the Yangtze River Delta is mostly mountainous and forest land and therefore difficult to develop and utilize. In addition, from 1980 to 2020, the spatial pattern of cultivated land and woodland did not change much, while construction land underwent a major change. Construction land was mainly scattered in the northern part of the Yangtze River Delta in 1980, while the area of construction land has increased significantly, showing a clump shape in 2020, especially in Shanghai and its surrounding cities. Moreover, the increase in cultivated land in the cities in southern Jiangsu Province is more than in the cities in northern Jiangsu Province. Additionally, the changes in cultivated land in various cities in Zhejiang Province is relatively even. Since the reform and opening up, with economic development and the increase in population, people continue to carry out large-scale development and construction, resulting in a continuous increase in the construction area. In some big cities, such as Shanghai, Suzhou, Nanjing, and Hangzhou, the large-scale increase in construction land has also

Table 3 Statistics of land use changes on the Yangtze River Delta from 1980 to 2020

Land-use type	Area (km ²)		Area Ratio (%)		1980–2020 Change (%)
	1980	2020	1980	2020	
Cultivated land	193684.586	170486.468	55.044	48.451	-11.98
Woodland	99819.485	102310.096	28.368	29.076	2.500
Grassland	13209.062	10802.288	3.754	3.070	-18.22
Water	24600.761	25568.043	6.991	7.266	3.932
Construction land	20490.511	42346.610	5.823	12.035	106.66
Unused land	67.635	358.536	0.019	0.102	430.10

The impact of land use/cover change on extreme temperatures on the Yangtze River Delta, China

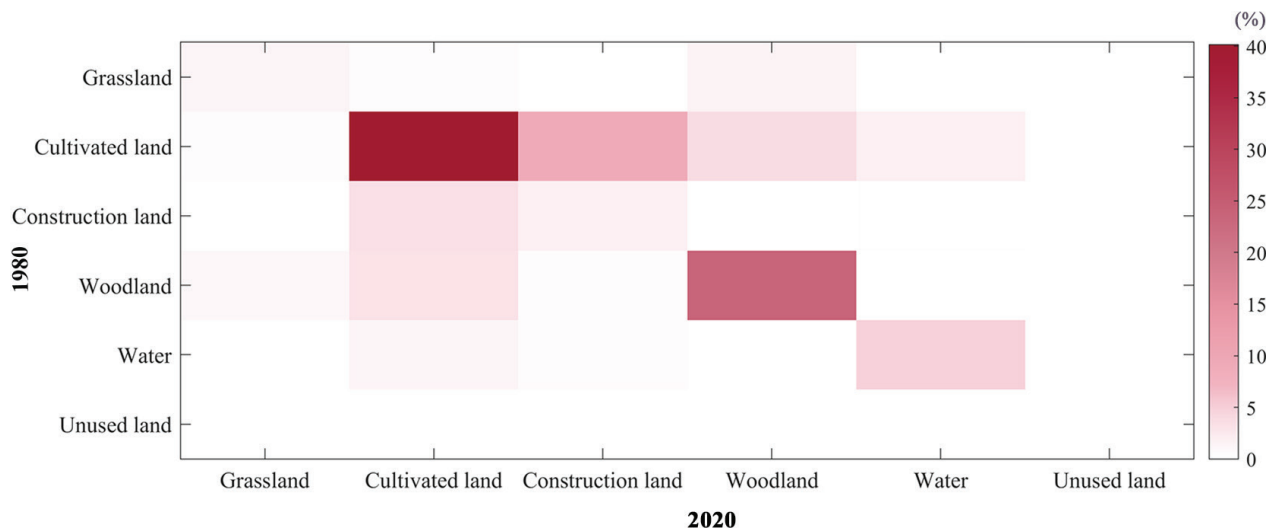


Fig. 5 Proportion of land-use type spatial transfer area on the Yangtze River Delta from 1980 to 2020. Source: own drawing based on the research results

increased the local impervious surface. Its increase makes the urban heat storage capacity increase, the water storage capacity poor, and airflow conduction blocked, seriously affecting the urban surface hydrological cycle, energy distribution, and the urban microclimate, resulting in the urban heat island effect, leading to a rapid increase in temperature in dense urban areas (Zhou and Hong 2018). From the land use changes (Fig. 6c), it can be seen that the area of construction land increased the most, mainly from the conversion of cultivated land. In addition, the conversion of cultivated land into woodland and the conversion of construction land into cultivated land is also relatively large. The smallest area of land use changes is the conversion of unused land to grassland.

3.3 Impact of LUCC on extreme temperatures

3.3.1 Contribution rate

The contribution rate of OMR can partially explain the degree of influence of surface forcing such as LUCC on temperature changes. The contribution rates of EHT and ELT in the Yangtze River Delta from 1980 to 2020 are shown in Table 4. In terms of annual changes, the contribution rate of LUCC on the annual extremely low temperatures is 92.4%, which is higher than the contribution rate of LUCC on the annual extremely high temperatures, indicating that ELT is more sensitive to LUCC, while EHT is less sensitive to LUCC.

Among the four seasons, extremely high temperatures trends are more pronounced in winter, with autumn having the weakest effect. The corresponding contribution rate is also the largest in winter, reaching 70.6%, followed by summer and spring, with contribution rates of 49.5% and 18.1%, respectively, with the smallest in autumn, with a contribution rate of 2.0%, indicating that the EHT increase in winter is mainly caused by the changes in land use type, while the EHT increase in autumn is less affected by the change in land use type. In winter, due to the wilting of surface vegetation, less transpiration and evaporation of soil moisture, and limited heat absorption, the OMR of EHT has an obvious upward trend (Li et al. 2008). Among the four seasons, ELT has the largest trends in autumn, with the smallest in spring. The corresponding contribution rate is also the largest in autumn, reaching 63.0%, followed by winter and summer, with contribution rates of 48.0% and 25.1%, respectively, and the smallest contribution rate of 7.1% is in spring. It shows that the change in land use in autumn has had the greatest impact on increasing ELT and has also had a certain impact on ELT in spring, summer, and winter, reaching more than 7%.

The impact of land use/cover change on extreme temperatures on the Yangtze River Delta, China

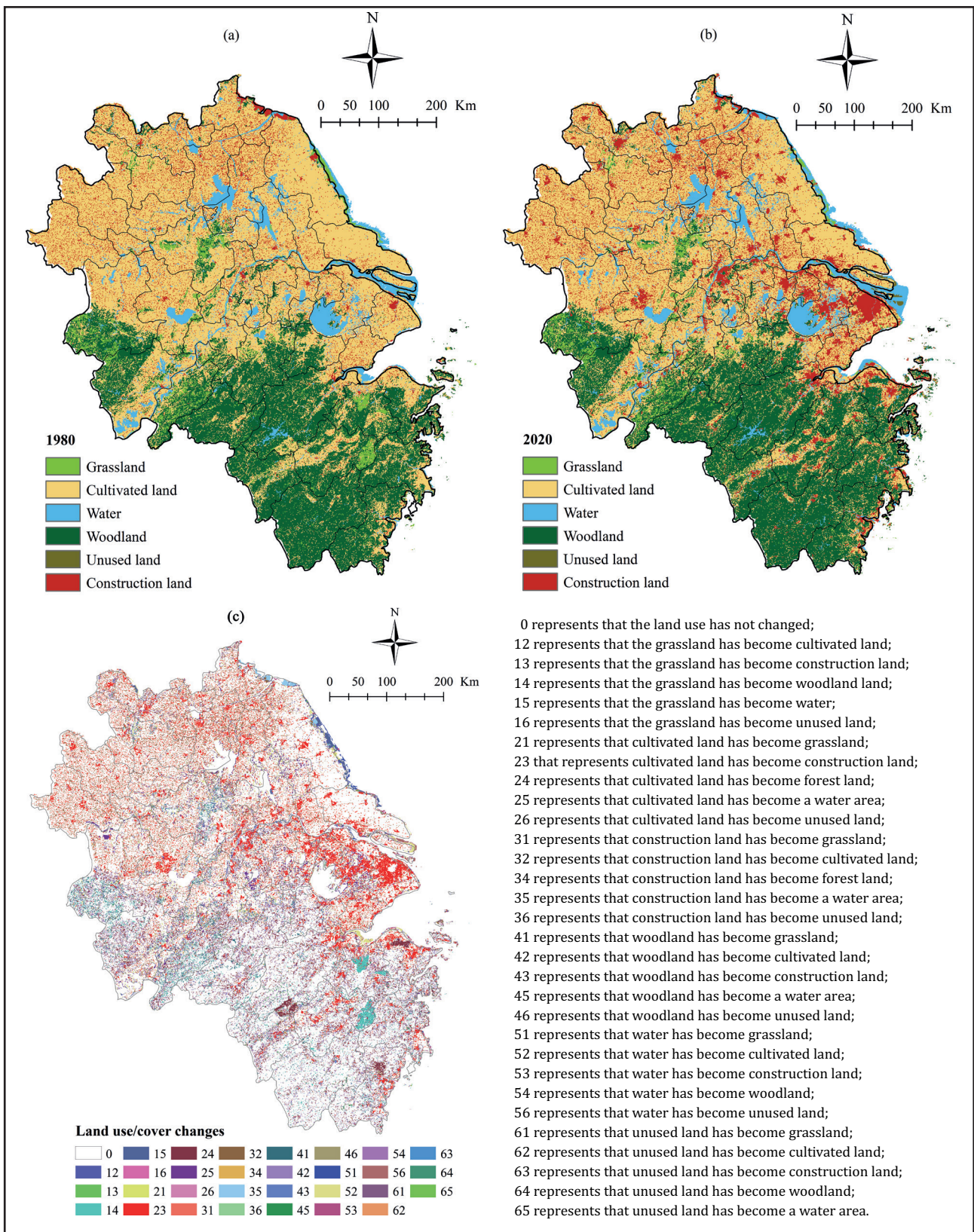


Fig. 6 Land use/cover: (a) 1980; (b) 2020; and (c) land use/cover changes from 1980 to 2020 on the Yangtze River Delta. Source: own drawing based on the research results

The impact of land use/cover change on extreme temperatures on the Yangtze River Delta, China

Table 4 Linear trend of OMR and contribution rates on the Yangtze River Delta in 1980–2020

OMR	Temperature	Annual	Spring	Summer	Autumn	Winter
Linear trend (°C/10a)	Extremely high temperatures	0.222	0.044	0.074	0.001	0.084
	Extremely low temperatures	0.517	0.012	0.031	0.098	0.065
Contribution Rate (%)	Extremely high temperatures	53.616	18.140	49.539	1.967	70.607
	Extremely low temperatures	92.355	7.121	25.139	62.969	47.957

3.3.2 Correlation

In order to further investigate the relationship between LUCC and extremely high/low temperatures, we calculated the correlation coefficients between NDVI and extremely high/low temperatures from the perspectives of interannual and monthly time scales. There are many factors that affect NDVI (Shi and Chen 2018), and LUCC can greatly affect the changes in NDVI (Guerschman et al. 2003). Therefore, the following results may explain only part of the impact of LUCC because NDVI was used as an indicator of LUCC in this study (Guerschman et al. 2003; Jung and Chang 2015; Xu et al. 2016).

Figure 7 shows the spatial distribution of the correlation coefficient between NDVI and the extremely high/low temperature indices at the interannual scale in the Yangtze River Delta during 1980–2020. In general, the absolute value of the interannual correlation coefficient between NDVI and extremely high/low temperatures in most stations is below 0.3, generally showing a weak correlation. The absolute value of the correlation coefficient in individual sites is between 0.3 and 0.6, reaching a relatively strong correlation. It is worth noting that most of the stations did not pass the significance test whether it was a correlation between EHT and NDVI or a correlation between ELT

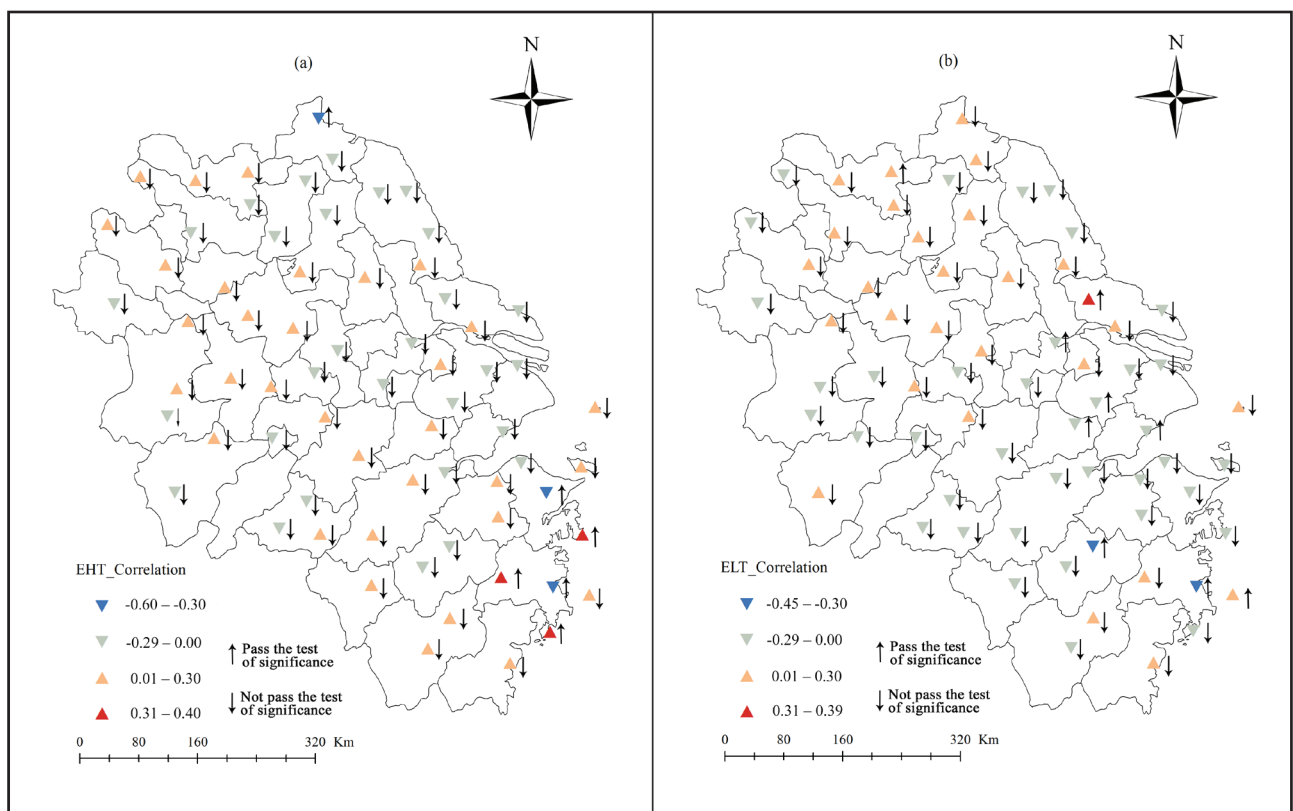


Fig. 7 Spatial distribution of correlation coefficients between NDVI and extremely high/low temperatures at the interannual time scale in the Yangtze River Delta during 1980–2020. Source: own drawing based on the research results

and NDVI. Specifically, on an interannual scale, the negative and positive correlations between NDVI and EHT are staggered, and the distribution is relatively uniform (Figure 7a). The difference is that the positive correlations between NDVI and ELT are mainly distributed in the north of the Yangtze River Delta, while the negative correlations between NDVI and ELT are mainly distributed in the south of the Yangtze River Delta (Fig. 7b), with a station ratio of 59%.

Figure 8 shows the spatial distribution of correlation coefficients between NDVI and EHT and the correlation coefficient between NDVI and ELT at the monthly

time scale in the Yangtze River Delta during 1980–2020. Their spatial patterns show extremely high similarities. Most of the absolute values of the monthly time scale correlation coefficients between NDVI and extremely high/low temperatures of each station are above 0.5, which are generally greater than the annual time scale correlation coefficients, which belong to a relatively strong correlation. In addition, most of the stations passed the significance test whether it was a correlation between EHT and NDVI or a correlation between ELT and NDVI. In addition, the correlation coefficients of only two stations, which are located on the islands in the southeast, failed the significance test.

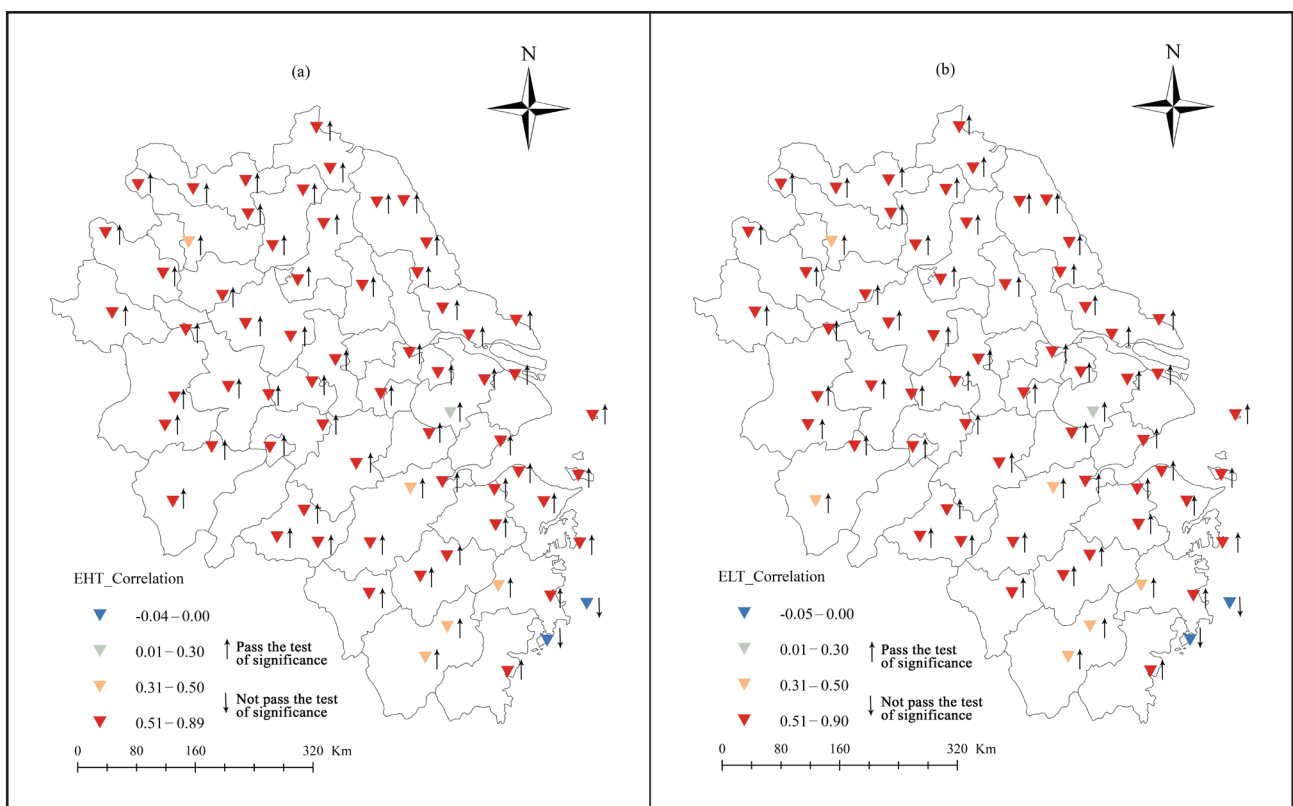


Fig. 8 Spatial distribution of correlation coefficient between NDVI and extremely high/low temperatures at the monthly time scale in the Yangtze River Delta during 1980–2020. Source: own drawing based on the research results

4. Discussion

In this study, we explored the impact of LUCC on EHT and ELT over the Yangtze River Delta during 1980–2020 by subtracting the reanalysis temperature from observed temperature (observation minus reanalysis (OMR) method) and the correlation analysis method. Different from the linear trend analysis of extremely high/low temperatures in previous studies, we found that extremely high/low temperatures shows a non-linear trend. EHT showed an upward trend during 1980–2008 and gradually declined after 2008, while ELT showed an upward trend during 1980–2020. We also found that EHT has a monthly time scale (quasi-3-month), inter-annual time scale (quasi-1-year, quasi-2-year, quasi-3-year and quasi-5-year), and inter-decadal scale (quasi-10 and quasi-35-year). ELT has a monthly time scale (quasi-3-month), inter-annual time scale (quasi-1-year, quasi-2-year, quasi-3-year and quasi-6-year), and inter-decadal time scale (quasi-10 and quasi-20-year). Although changes in extreme temperatures is complicated, the change is not random, but has periodicity. In addition, the spatial patterns of EHT and ELT are quite different, and there is also spatial heterogeneity within each. These results are of great significance for understanding extreme temperature changes from the perspective of multiple time scales and nonlinearity.

In this work, characteristics of LUCC on the Yangtze River Delta showed that a decrease in cultivated land and an increase in constructed land are the most obvious characteristics of LUCC. There are two reasons for cultivated land degradation: on the one hand, the increase in construction land is the most common reason for the decrease in cultivated land; on the other hand, the loss of cultivated land caused by the acceleration of the adjustment of the internal structure of cultivated land and the increase in the area of woodland and grassland cannot be ignored. Meanwhile, related research has also concluded that the cultivated land in the Yangtze River Delta is gradually decreasing, and the contradiction between people and cultivated land has become more serious (Chen et al. 2009; Yuan et al. 2019). With economic and social development on the Yangtze River Delta, the improvement of people's living standards and the influx of large amounts of foreign capital and talents, the process of urbanization has accelerated. People's demand for residential and commercial housing has increased sharply, and the land resources required for real estate development have also increased significantly. The expansion of

construction land is achieved through the encroachment of high-quality garden plots, vegetable plots, paddy fields and other cultivated land resources on the outskirts of the city, leading to a year-to-year decrease in the area of cultivated land, intensifying the contradiction between people and land, and triggering a series of social problems (Chen et al. 2009). Therefore, it is important to coordinate the relationship between cultivated land and construction land.

We further attempted to investigate the LUCC's linkage with the extreme temperature changes over the Yangtze River Delta during 1980–2020. The analysis results indicated that land use changes during 1980–2020 led to EHT warming of 0.39°C per decade and ELT warming 0.53°C per decade over the Yangtze River Delta during this period. In addition, the contribution rates of LUCC on EHT and ELT were 53.6% and 92.4%, respectively. Many scholars have used the OMR method to analyze and study regional temperature changes based on LUCC. For instance, Zhou et al. (2004) found that the contribution rates of LUCC on average maximum temperature and average minimum temperature were 5% and 21%, respectively, in the southeast of China during 1979–1998 based on NCEP/NCAR R1 reanalysis. Zhang et al. (2005) analyzed the contribution rate of LUCC on the average temperature, average maximum temperature, and average minimum temperature in the area east of 110°E in China based on R1 reanalysis datasets and pointed out that the contribution rates of LUCC on them were 18%, 5%, and 29% during 1960–1999. Yang et al. (2011) explored the impact of LUCC on average temperature in eastern China, and the result showed that the contribution rate was 24.2% during 1980–2007. The contribution from LUCC toward the temperature in recent decades is of great concern across the globe. Several studies (Betts et al. 2007; Rounsevell and Reay 2009) have also highlighted that LUCC largely regulates the lower atmosphere and thus influences the climate over a region. Our results are different from previous studies, which mainly discuss the influence of LUCC on average temperature, and ignore the influence of LUCC on extreme temperatures. Our research started from the perspective of extreme temperatures and found that the impact of LUCC on extreme temperature is greater than the impact of LUCC on average temperature (40%) in China found in previous studies (Hu et al. 2010), and the impact on ELT is greater than that on EHT. The results will be useful for enhancing our knowledge in the context of the impact of LUCC on extreme temperatures over the Yangtze

River Delta and for understanding the impact of LUCC on temperature from multiple perspectives.

From the correlation results between NDVI and extremely high/low temperatures, compared with the annual time scale response characteristics, the monthly time scale response of NDVI to extreme temperatures is more regionally concentrated in spatial distribution. The reason is that, on the one hand, the annual scale correlation between NDVI and extreme temperatures reflects the correlation between the long-term trends of the two. This correlation fails to “stretch” other factors, such as the effects of urbanization, irrigation, artificial afforestation, and solar radiation on vegetation growth. On the other hand, the monthly scale correlation is a correlation analysis based on a nearly stationary data series after de-seasonalization, which may eliminate signals with seasonal changes to a certain extent such as precipitation, solar radiation, and regular agricultural production, which is a more scientific and reasonable way to explore the relationship between NDVI and extreme temperatures. The NDVI is mostly positively correlated with extremely high/low temperatures, indicating that the increase in temperature is beneficial to the growth of vegetation in the Yangtze River Delta. The region is relatively rich in water resources, and the evapotranspiration caused by the rising temperature will take away excess water and then promote the growth of vegetation. Therefore, extreme temperatures, especially the increase of ELT, promotes the growth of vegetation in the Yangtze River Delta. However, related studies (*Wang and Hou 2019*) point out that extreme temperatures are negatively correlated with NDVI, i.e., the increase in extreme temperatures will inhibit the growth of vegetation in North China. It can be seen that there is large spatial heterogeneity in the relationship between NDVI and extreme temperatures, which requires us to conduct specific analyses on different regions.

5. Conclusions

This study mainly explored the impact of LUCC on extreme temperatures during 1980–2020 on the Yangtze River Delta. We first analyzed the spatio-temporal changes of extremely high temperatures and extremely low temperatures by using the EEMD and EOF methods. Then, the spatio-temporal changes of LUCC during 1980–2020 were also discussed. Finally, we investigated the impact of LUCC on extremely

high/low temperatures by using the OMR and correlation analysis methods in the Yangtze River Delta. The main conclusions of this study can be summarized as follows.

1. Extreme temperatures showed a non-linear trend during 1980–2020. EHT has a monthly time scale (quasi-3-month), inter-annual time scale (quasi-1-year, quasi-2-year, quasi-3-year and quasi-5-year), and inter-decadal scale (quasi-10 and quasi-35-year). ELT has a monthly time scale (quasi-3-month), inter-annual scale (quasi-1-year, quasi-2-year, quasi-3-year and quasi-6-year), and inter-decadal scale (quasi-10 and quasi-20-year). In space, EHT and ELT and their respective internal spatial patterns have obvious heterogeneity, where EHT mainly showed an east-middle-west staggered phase and ELT showed a southeast-northwest anti-phase pattern.
2. The decrease in cultivated land and the increase in constructed land are the most obvious characteristics of LUCC, and the proportion of cultivated land transferred to construction land was the largest. Unused land showed the least change during 1980–2020. The decrease in cultivated land has exacerbated the human–land contradiction in the Yangtze River Delta. In future land use planning, it is necessary to coordinate the relationship between cultivated land and construction land.
3. The contribution rates of LUCC on extremely high temperatures and extremely low temperatures are 53.6% and 92.4%, respectively, which is higher than for the average temperature. The increase in extremely high/low temperatures is mainly due to changes in local land use.
4. At the monthly time scale the response of NDVI to extreme temperatures is more regionally concentrated than that on the interannual time scale in spatial distribution. In addition, there is a significant positive correlation between extremely high/low temperatures and NDVI in most regions. The increase in extreme temperatures is conducive to the growth of vegetation.

Author contributions

Conceptualization, N.N.Z.; methodology, N.N.Z.; software, H.Q.Y., D.H.L and M.Y.Z; validation, H.Q.Y.; formal analysis, N.N.Z; investigation, N.N.Z; resources, H.Q.Y.; data curation, H.Q.Y.; writing: original draft preparation, N.N.Z.; writing: review and editing, N.N.Z. and H.Q.Y.; visualization, N.N.Z. All authors have read and agreed to the published version of the manuscript.

Data availability statement

The data presented in this study are openly available in Data Center for Resources and Environmental Sciences, Chinese Academy of Sciences (RESDC), <http://www.resdc.cn/DOI/DOI.aspx?DOIid=49> (accessed on 3 May 2021, doi:10.12078/2018060601, reference number Xu 2018).

Acknowledgments

This research was funded by the Shanghai Sailing Program (Grant No. 22YF1411000) and the Doctoral research program (Grant No. 21E021) of China West Normal University. We gratefully acknowledge financial support from the National Nature Science Foundation of China (Grant No. 42130510).

References

- Avila, F.B., A.J. Pitman, M.G. Donat, L.V. Alexander and G. Abramowitz 2012: Climate model simulated changes in temperature extremes due to land cover change. – *Journal of Geophysical Research: Atmospheres* **117** (D4): 1-19, doi:10.1029/2011JD01
- Bai, L., Z. Liu, Z. Chen and J. Xu 2017: Runoff nonlinear variation and responses to climate fluctuation in the headwater region of the Kaidu River. – *Resources Science* **39** (8): 1511-1521, doi:10.18402/resci.2017.08.08
- Betts, R.A., P.D. Faloon, K.K. Goldewijk and N. Ramanketty 2007: Biogeophysical effects of land use on climate: Model simulations of radiative forcing and large-scale temperature change. – *Agricultural and Forest Meteorology* **142** (2-4): 216-233, doi:10.1016/j.agrformet.2006.08.021
- Chen, H., J. Cui and J. Chen 2009: The Driving Mechanism of Cultivated Land Quantity Change and Performance of Relative Policies in Yangtze River Delta (in Chinese). – *Resources Science* **31** (5): 807-815
- Chen, Z., Y. Chen, L. Bai and J. Xu 2017: Multiscale evolution of surface air temperature in the arid region of Northwest China and its linkages to ocean oscillations. – *Theoretical and Applied Climatology* **128** (3-4): 945-958, doi:10.1007/s00704-016-1752-7
- China Meteorological Administration 2011: Classification and Coding of Meteorological Elements (QX/T 133-2011). – Online available at: <http://data.cma.com>, accessed 28/12/2019
- Davin, E.L., S.I. Seneviratne, P. Ciais, A. Olioso and T. Wang 2014: Preferential cooling of hot extremes from cropland albedo management. – *Proceedings of the National Academy of Sciences* **111** (27): 9757-9761, doi:10.1073/pnas.1317323111
- Friedl, M. and D. Sulla-Menashe 2015: MCD12C1 MODIS/Terra+Aqua Land Cover Type Yearly L3 Global 0.05Deg CMG V006. NASA EOSDIS Land Processes DAAC. – Online available at: <http://www.modis.gsfc.nasa.gov>, accessed 20/11/2019
- Gogoi, P.P., V. Vinoj, D. Swain, G. Roberts, J. Dash and S. Tripathy 2019: Land use and land cover change effect on surface temperature over Eastern India. – *Scientific Reports* **9** (1): 1-10, doi:10.1038/s41598-019-45213-z
- Gu, C., L. Hu, X. Zhang and G. Jing 2011: Climate change and urbanization in the Yangtze River Delta. – *Habitat International* **35** (4): 544-552, doi:10.1016/j.habitatint.2011.03.002
- Guerschman, J., J. Paruelo and I. Burke 2003: Land use impacts on the Normalized Difference Vegetation Index in temperate Argentina. – *Ecological Application* **13** (3): 616-628, doi:10.1890/1051-0761(2003)013[0616:luiotn]2.0.co;2
- Hu, Y., W. Dong and Y. He 2010: Impact of land surface forcings on mean and extreme temperature in eastern China. – *Journal of Geophysical Research: Atmosphere* **115** (D19): 1-11, doi:10.1029/2009jd013368
- IPCC (Intergovernmental Panel on Climate Change) 2013: Climate Change 2013: The Physical Science Basis. Contribution of Working Group I to the Fifth Assessment Report of the Intergovernmental Panel on Climate Change. – Cambridge/New York
- Jung, M. and E. Chang 2015: NDVI-based land-cover change detection using harmonic analysis. – *International Journal of Remote Sensing* **36** (4): 1097-1113, doi:10.1080/01431161.2015.1007252
- Karl, T.R., N. Nicholls and A. Ghazi 1999: CLIVAR/GCOS/WMO workshop on indices and indicators for climate extremes: Workshop summary. – *Climatic Change* **42**: 3-7, doi:10.1007/978-94-015-9265-9_2
- Kistler, R., W. Collins, D. Deaven, L. Gandin, M. Iredell, S. Saha, G. White, J. Woollen, Y. Zhu, M. Chelliah, W. Ebisuzaki, W. Higgins, J. Janowiak, K.C. Mo, C. Ropelewski, J. Wang, A. Leetmaa, R. Reynolds, R. Jenne and D. Joseph 2001: NCEP/NCAR reanalysis data. – Online available at: <https://psl.noaa.gov/data/gridded/reanalysis/>, accessed online

11/05/2019

- Li, Y., Y. Wang, H. Chu and J.P. Tang 2008: The climate influence of anthropogenic land-use changes on near-surface wind energy potential in China. – *Science Bulletin* **53** (18): 2859-2866, doi:10.1007/s11434-008-0360-z
- Liu, H., Q. Zhan, C. Yang and J. Wang 2019: The multi-time-scale temporal patterns and dynamics of land surface temperature using Ensemble Empirical Mode Decomposition. – *Science of the Total Environment* **652**: 243-255, doi:10.1016/j.scitotenv.2018.10.252
- Luber, G. and M. McGeehin 2008: Climate change and extreme heat events. – *American Journal of Preventive Medicine* **35** (5): 429-435, doi:10.1016/j.amepre.2008.08.021
- Nori-Sarma, A., G.B. Anderson, A. Rajiva, G. Shah-Azhar, P. Gupta, M.S. Pednekar, J. Young Son, R.D. Peng and M.L. Bell 2019: The impact of heat waves on mortality in North-west India. – *Environmental Research* **176**: 108546, doi:10.1016/j.envres.2019.108546
- North, G.R., T.L. Bell, R.F. Cahalan and F.J. Moeng 1982: Sampling errors in the estimation of empirical orthogonal functions. – *Monthly weather review* **110** (7): 699-706
- Orlowsky, B. and S.I. Seneviratne 2012: Global changes in extreme events: regional and seasonal dimension. – *Climatic Change* **110** (3-4): 669-696, doi:10.1007/s10584-011-0122-9
- Pitman, A.J., N. de Noblet-Ducoudré, F.B. Avila, A.V. Alexander, J.P. Boisier, V. Brovkin, C. Delire, F. Cruz, M.G. Donat, V. Gayler, B. van den Hurk, C. Reick and A. Voldoire 2012: Effects of land cover change on temperature and rainfall extremes in multi-model ensemble simulations. – *Earth System Dynamics* **3** (2): 213-231, doi:10.5194/esd-3-213-2012
- Qian, W. and B. Lu 2010: Periodic oscillations in millennial global mean temperature and their cause. – *Chinese Science Bulletin* **55** (35): 4052-4057, doi:10.1007/s11434-010-4204-2
- Qin, Z., X. Zou and F. Weng 2012: Comparison between linear and nonlinear trends in NOAA-15 AMSU-A brightness temperatures during 1998–2010. – *Climate Dynamics* **39** (7-8): 1763-1779, doi:10.1007/s00382-012-1296-1
- Rounsevell, M. and D.S. Reay 2009: Land use and climate change in the UK. – *Land Use Policy* **26** (S1): S160-S169, doi:10.1016/j.landusepol.2009.09.007
- Sang, Y.F. 2012: Spatial and temporal variability of daily temperature in the Yangtze River Delta, China. – *Atmosphere Research* **112** (1): 12-24, doi:10.1016/j.atmosres.2012.04.006
- Shi, H. and J. Chen 2018: Characteristics of climate change and its relationship with land use/cover change in Yunnan Province, China. – *International Journal of Climatology* **38** (5): 2520-2537, doi:10.1002/joc.5404
- Sun, Y., X. Zhang, F.W. Zwiers, L. Song, H. Wan, T. Hu and G. Ren 2014: Rapid increase in the risk of extreme summer heat in Eastern China. – *Nature Climate Change* **4** (12): 1082, doi:10.1038/nclimate2410
- Tang, D., M. Mao, J. Shi and W. Hua 2021: The Spatio-Temporal Analysis of Urban-Rural Coordinated Development and Its Driving Forces in Yangtze River Delta. – *Land* **10** (5): 495, doi:10.3390/land10050495
- Tebaldi, C., K. Hayhoe, J.M. Arblaster and G.A. Meehl 2006: Going to the extremes. – *Climate Change* **79** (3): 185-211, doi:10.1007/s10584-006-9051-4
- Teuling, A.J., S.I. Seneviratne, R. Stöckli, M. Reichstein, E. Moors, P. Ciais, S. Luyssaert, B. van den Hurk, C. Ammann, C. Bernhofer, E. Dellwik, D. Gianelle, B. Gielen, T. Grünwald, K. Klumpp, L. Montagnani, C. Moureaux, M. Sottocornola and G. Wohlfahrt 2010: Contrasting response of European forest and grassland energy exchange to heatwaves. – *Nature Geoscience* **3** (10): 722-727, doi:10.1038/ngeo950
- The National Center for Atmospheric Research 2018: Global GIMMS NDVI3g v1 dataset (1981–2015). National Tibetan Plateau/Third Pole Environment Data Center. – Online available at: <http://www.tpc.ac.cn>, assessed at 12/06/2019
- Turaner, B.L.I., R.H. Moss and D.L. Skole 1993: Relating land use and global land-cover change: a proposal for an IGBP-HDP core project. – A report from the IGBP/HDP Working Group on Land-Use/Land-Cover Change. – Stockholm
- Wang, J., Z. Yan, P.D. Jones and J. Xia 2013: On ‘observation minus reanalysis’ method: A view from multidecadal variability. – *Journal Geophysical Research: Atmosphere* **118** (4): 7450-7458, doi:10.1002/jgrd.50574
- Wang, X. and X. Hou 2019: Variation of Normalized Difference Vegetation Index and its response to extreme climate in coastal China during 1982-2014. – *Geographical Research* **38** (04): 69-83
- Wilhelm, M., E.L. Davin and S.I. Seneviratne 2015: Climate engineering of vegetated land for hot extremes mitigation: An Earth system model sensitivity study. – *Journal of Geophysical Research: Atmospheres* **120** (7): 2612-2623, doi:10.1002/2014JD022293
- Wu, Z. and N.E. Huang 2011: Ensemble Empirical Mode Decomposition: A Noise-Assisted Data Analysis Method. – *Advances in Adaptive Data Analysis* **1** (1): 1-41, doi:10.1142/S1793536909000047
- Xu, L., B. Li, Y. Yuan, X. Gao, T. Zhang and S. Qingling, S. 2016: Detecting different types of directional land cover changes Using MODIS NDVI time series dataset. – *Remote Sensing* **8** (6): 495, doi:10.3390/rs8060495
- Xu, X. 2018: China Annual Vegetation Index (NDVI) Spatial Distribution Dataset. – Data Registration and Publishing System of the Resource and Environmental Science Data Center of the Chinese Academy of Sciences. – Online available at: <http://www.resdc.cn/DOI>, accessed 03/5/2021

The impact of land use/cover change on extreme temperatures on the Yangtze River Delta, China

- Yang, H., X. Zhong, S. Deng and H. Xu 2021: Assessment of the impact of LUCC on NPP and its influencing factors in the Yangtze River basin, China. – *Catena* **206** (1-2): 105542, doi:10.1016/j.catena.2021.105542
- Yang, X., Y. Hou and B. Chen 2011: Observed surface warming induced by urbanization in east China. – *Journal of Geophysical Research: Atmosphere* **16** (D14): 1-12, doi:10.1029/2010JD015452
- Yao, J., Z. Liu, Q. Yang, Y. Liu, C. Li and W. Hu 2014: Temperature variability and its possible causes in the typical basins of the arid Central Asia in recent 130 years. – *Acta Geographica Sinica* **69** (3): 291-302, doi:10.11821/dlxb201403001
- Yuan, J., Y. Xu, J. Xiang, L. Wu and D. Wang 2019: Spatiotemporal variation of vegetation coverage and its associated influence factor analysis in the Yangtze River Delta, eastern China. – *Environmental Science and Pollution Research* **26** (32): 32866-32879, doi:10.1007/s11356-019-06378-2
- Zhang, B. and W. Zhou 2021: Spatial-Temporal Characteristics of Precipitation and Its Relationship with Land Use/Cover Change on the Qinghai-Tibet Plateau, China. – *Land* **10**: 1-21, doi:10.3390/land10030269
- Zhang, J., W. Dong, L. Wu, J. Wei and P. Chen 2005: Impact of Land Use Changes on Surface Warming in China. – *Advances in Atmospheric Sciences* **022** (3): 343-348, doi:10.1007/BF02918748
- Zhang, X., L. Alexander, G. Hegerl, P. Jones, A. Tank, T. Peterson, B. Trewin and F. Zwiers 2011: Indices for monitoring changes in extremes based on daily temperature and precipitation data. – *Wiley Interdisciplinary Reviews: Climate Change* **2** (6): 851-870, doi:10.1002/wcc.147
- Zhou, L., R.E. Dickinson, Y. Tian, J. Fang, Q. Li, R.K. Kaufmann, C.J. Tucker and R.B. Myneni 2004: Evidence for a significant urbanization effect on climate in China. – *Proceeding of the National Academy of Sciences* **101** (26): 9540-9544, doi:10.1073/pnas.0400357101
- Zhou, X. and C. Hong 2018: Impact of urbanization-related land use land cover changes and urban morphology changes on the urban heat island phenomenon. – *Science of the Total Environment* **635** (9): 1467-1476, doi:10.1016/j.scitotenv.2018.04.091
- Zhu, N., J. Xu, K. Li, Y. Luo and C. Zhou 2019a: Spatiotemporal Change of Plum Rains in the Yangtze River Delta and Its Relation with EASM, ENSO, and PDO During the Period of 1960–2012. – *Atmosphere* **10** (5): 258, doi:10.3390/atmos10050258
- Zhu, N., J. Xu, C. Wang, Z. Chen and Y. Luo 2019b: Modeling the multiple time scale response of hydrological drought to climate change in the data-scarce inland river basin of Northwest China. – *Arabian Journal of Geosciences* **12** (7): 1-16, doi:10.1007/s12517-019-4404-2